Vision Research 50 (2010) 838–849

Contents lists available at ScienceDirect

Vision Research

journal homepage: www.elsevier.com/locate/visres

The horizontal effect in suppression: Anisotropic overlay and surround suppression at high and low speeds

Yeon Jin Kim, Andrew M. Haun [1], Edward A. Essock *

Department of Psychological and Brain Sciences, University of Louisville, Louisville, KY 40292, USA

ARTICLE INFO

Article history:
Received 16 June 2009
Received in revised form 25 January 2010

Keywords:
Surround suppression
Overlay suppression
Contrast gain control
Horizontal effect
Contrast normalization
Natural scenes
Oblique effect
Masking
Sustained and transient

ABSTRACT

When a pattern of broad spatial content is viewed by an observer, the multiple spatial components in the pattern stimulate detecting-mechanisms that suppress each other. This suppression is anisotropic, being relatively greater at horizontal, and least at obliques (the "horizontal effect"). Here, suppression of a grating by a naturalistic (1/*f*) broadband mask is shown to be larger when the broadband masks are temporally similar to the target's temporal properties, and generally anisotropic, with the anisotropy present across all spatio-temporal parings tested. We also show that both suppression from within the region of the test pattern (overlay suppression) and from outside of this region (surround suppression) show the horizontal-effect anisotropy. We conclude that these suppression effects stem from locally-tuned and anisotropically-weighted gain-control pools.

1. Introduction

Visual processing of images that contain a broad spectrum of content (e.g., 1/*f* or natural scenes) is anisotropic (Essock, DeFord, Hansen, & Sinai, 2003; Essock, Haun, & Kim, 2009; Hansen & Essock, 2004; Hansen & Essock, 2005; Hansen & Essock, 2006; Hansen, Essock, Zheng, & DeFord, 2003). When viewing broadband images, people find oblique content to be much more salient and horizontal content to be least so, with vertical content intermediate. Similarly, thresholds for oblique content in broadband images are lowest and thresholds are highest for horizontal content. There is strong evidence that this "horizontal effect" is due to anisotropic contrast gain control that provides less suppression at oblique orientations and most suppression at horizontal (e.g., Essock et al., 2009). When a grating pattern is viewed in isolation, without a broadband background to drive the anisotropic gain-control mechanism, oblique content is seen *least* well (the "oblique effect"). Although the contrast response function for a grating (i.e., from threshold vs. contrast (TvC) functions) is equivalent at all orientations once beyond the near-threshold region where the oblique effect is observed (Essock et al., 2009), when a broadband mask is present the effect of anisotropic gain-control suppression is observed in the TvC functions for different orientations (Haun & Essock, in preparation).

In the present study we again use 1/*f* random-phase noise to simulate the spatial context of viewing natural scenes. Here, we measure its masking effect at different orientations in specific spatio-temporal conditions in order to probe different detecting-mechanisms. We first consider the correspondence between the temporal characteristics of the target and (broadband) mask in the production of the anisotropy – specifically, whether a high-speed (temporally "transient") broadband pattern will anisotropically mask a low-speed (temporally "sustained") test grating, and vice versa. Snowden (2001); Hammett & Snowden, 1995) has shown the importance of the matching of temporal properties of test grating and a grating mask (i.e., narrowband mask), showing that masking is much stronger when a test grating with "sustained" temporal characteristics is masked by a sinewave mask also with "sustained" temporal properties (and likewise for "transient" tests and masks). Furthermore, Snowden (2001) has shown that in one case this masking is temporally sustained, occurring throughout the presentation of the mask, and in the other case the masking occurs at the temporal transients of mask onset and offset. In addition, studies employing a temporally-modulated narrowband mask have delineated temporal tuning of at least two mechanisms (Mandler & Makous, 1984; Fredericksen & Hess, 1998; Fredericksen & Hess, 1999; Anderson & Burr, 1985; Bex, Verstraten, & Mareschal, 1996; Boynton & Foley, 1999; Cass &

* Corresponding author.
E-mail address: essock@louisville.edu (E.A. Essock).
[1] Present address: Schepens Eye Research Institute Boston MA.

0042-6989/$ - see front matter © 2010 Elsevier Ltd. All rights reserved.
doi:10.1016/j.visres.2010.01.020

Alais, 2006) and their tuning suggests that masking should be greater when tests and masks are rather similar temporally than when they are very different (however, see Boynton & Foley, 1999). Assuming that broadband masking behaves like masking by a single grating, these prior results suggest that strongest broadband masking should also be seen when the spatial and temporal properties of a test and mask both strongly stimulate the same mechanism. If for test targets with very different spatio-temporal properties, masks with different temporal properties are differentially effective, multiple relatively-local gain-control pools would be indicated, raising the issue of whether all such pools are anisotropically weighted. In the first experiment, we assess whether detecting-mechanisms widely-separated on the spatial–temporal surface have distinct gain-control pools that show a horizontal-effect anisotropy.

A second issue addressed in this study was the nature of this anisotropy with respect to distinctly different types of suppression. Several authors have distinguished between suppression from a local region overlapping the test, termed "overlay" suppression, and "surround" suppression coming from within an annular region not covering the target location (Meese, Summers, Holmes, & Wallis, 2007; Petrov, Carandini, & McKee, 2005; Yu, Klein, & Levi, 2003). In our prior studies on the horizontal effect, we've considered a more general, "every-day", viewing situation where the spatial context is broadband, the pattern is centrally viewed, and the broadband mask covers a fairly large region (as when viewing a real-world object). That is, both the overlay and surround regions (of several spatially-distributed detectors) are covered by the broadband spatial context in the real-world and also by the 5–10° stimuli used previously in demonstrating the horizontal effect. In the second experiment, we consider whether this anisotropic masking comes from surround suppression, overlay suppression, or both, and whether either type of suppression mechanism occurs exclusively with either temporal transients or sustained presentations.

The goal of these experiments was to determine whether the horizontal effect could be localized to particular masking mechanisms. Our findings indicate that where significant broadband masking can be measured, by whatever presumed mechanism, a horizontal effect will also be observed. Thus, in general every-day viewing, the horizontal effect: is driven by contextual spatial structure similar to a particular filter's spatial and temporal tuning; is present for a range of spatial and temporal filters; and exists in both surround and overlay suppression.

2. Methods

2.1. General

A $1/f$ broadband noise spatial pattern was used to mask a grating target, and each mask and target was presented with either flickered (temporally-transient) or gradual (temporally sustained) temporal characteristics. The spatial frequency of the test grating was either 'low' (1 cpd at the fovea) or 'high' (8 cpd at the fovea). Masking was compared at horizontal, vertical and oblique orientations to evaluate the magnitude of the anisotropy ("horizontal effect") of suppression.

The configuration of the stimuli used in the experiments is shown in Fig. 1. Essentially, we tested with our "general-viewing" conditions in Experiment 1 (large broadband mask and test patch, foveal viewing) and evaluated temporal properties of the anisotropy; then in Experiment 2, stimulus sizes, configurations, and eccentricities were altered to evaluate the potential anisotropy of overlay suppression (Experiment 2.1) and surround suppression (Experiment 2.2) using conditions typical for evoking those two types of suppression (a smaller test patch and associated overlaid mask or contiguous annular mask).

2.2. Procedure and stimuli

2.2.1. Procedure

Each experiment used a 40-trial two-interval forced-choice (2IFC) QUEST procedure to estimate the 82%-correct contrast threshold for Gaussian-windowed sinewave grating targets (Gabors). Each trial consisted of two intervals, both containing an identical mask. One interval (randomly selected) also contained the target presented concurrently with the mask (see Fig. 1, right column). Both intervals contained either identical noise mask images or, in the baseline condition, an unpatterned mean-luminance background. (Thus except for the baseline condition, observers discriminated between the pattern in the middle column and the pattern in the column to the right in the same row, presented in the two intervals.) The subjects were asked to fixate a small circular centered spot present between trials and during the ISI (a 2-pixel-wide ring with an outer diameter of approximately 0.13°). In Experiment 1 targets were viewed foveally, whereas in Experiment 2 targets were either viewed foveally or at 2° to the left of fixation.

2.2.2. Temporal properties

The two intervals of each trial were separated by a 500 ms ISI, with trial duration depending on the temporal properties of each condition. Two temporal conditions were used: a "flickered" condition consisting of 16.7 Hz (12 frames per cycle) sinewave modulation windowed by a slow envelope, and a "gradual" condition consisting of a static pattern windowed with the same envelope. The envelope was either a slowly-ramped onset and offset (Experiment 1; see Fig. 2a) or a Gaussian envelope (Experiment 2; see Fig. 2b). The ramped waveform was 560 ms in duration (100 ms linear ramp from zero to nominal contrast, 360 ms plateau, and a 100 ms linear ramp to zero contrast). The Gaussian temporal envelope had a full width at half height of 400 ms (σ = 170 ms). Thus, the "flickered" and "gradual" stimuli had the same temporal envelope and the same peak contrast, but different time-averaged contrast (because the 'gradual' presentation was static rather than temporally counterphased).

2.2.3. Test stimuli

The grating target was presented at either 0°, 45°, 90°, or 135° clockwise from vertical. Target size (the width of the Gaussian window) was varied according to the demands of each condition: full width at half height of the target was 2° in Experiment 1, 1° in Experiment 2.1 and was $\lambda\sqrt{e}/\sqrt{2}$° in Experiment 2.2 (where λ is the wavelength of the grating). Target spatial frequencies were 1 or 8 cpd at fixation, and .6 or 4.8 cpd at 2° eccentricity.

2.2.4. Mask stimuli

The masks consisted of oriented broadband noise with the band of orientations present centered at the same orientation as the test grating. The spatial-frequency band used was four octaves, including spatial frequencies from 1 to 16 cpd, and the orientation bandwidth was 15°. The 384 × 384-pixel mask images were created by inverse Fourier transform of $1/f$ amplitude spectra, with random phase coefficients generated on each trial (but the same on the two intervals of a single trial), and multiplied by a rectangular bandpass filter in orientation (see Essock et al., 2003 or Hansen & Essock, 2003 for more details). The spatial aspects of the mask differed depending upon experimental condition (see below). Contrast of the mask in all conditions was set so that the standard deviation of normalized pixel luminances (ranging from 0 to 1), or root-mean-square contrast, was 0.10.

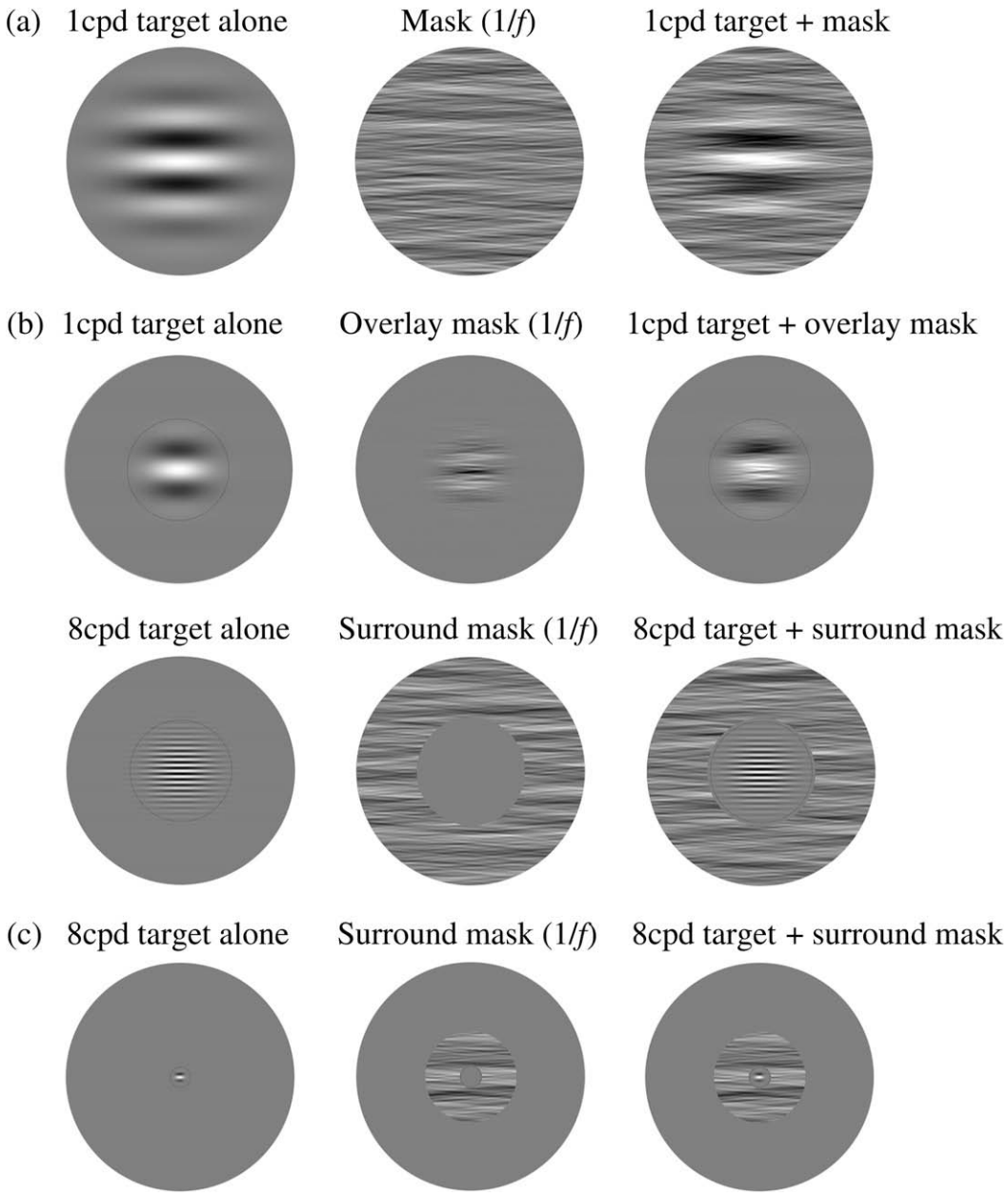

Fig. 1. Examples of the test target (left column), broadband oriented 1/*f* noise mask (middle column), and combined target and mask (right column) are shown, all rendered at the same scale. In the two intervals of a 2IFC trial, subjects had to discriminate between the stimuli in the middle and right columns (except on 'baseline' conditions, when there was no mask at all). The mean-luminance monitor screen surrounding the stimuli was truncated by a large circular window (usually 5°) and is shown to scale indicated by the extent of these circular patches. Row 'a' shows an example of the stimuli for Experiment 1. Panel 'b' shows an example for Experiment 2.1 with the upper row showing the overlay mask and the lower row showing the surround mask condition. Row 'c' shows an example (8 cpd target at fixation) of the stimuli for Experiment 2.2.

2.2.5. Apparatus

The stimuli were displayed on a monochrome M21LMAX Image Systems, Inc. CRT monitor (white P104 phosphor). A video attenuator (built by Vision Research Graphics, Inc.) was used to present a linear luminance range providing a grayscale resolution greater than 2^{12} luminance levels. Matlab 7.4, with the Psychophysics Toolbox extensions, was used to design the experiments and present stimuli. Mean luminance of the display was 30 cd/m^2, resolution was set to 800 × 600 pixels, and refresh rate was 200 Hz. Viewing distance was 1.92 m in Experiments 1 and 2.1. In Experiment 2.2, viewing distance varied with target spatial frequency (see below). Stimuli were viewed in a darkened room through a 5°-diameter circular aperture in a large circular surround 27° in diameter (when viewed from 1.92 m) affixed to the monitor (which obscured the monitor bezel and other nearby contours).

2.2.6. Observers

There were three observers in each experiment. One of the authors and a second observer participated in all three experiments and three additional observers each participated in one experiment. All subjects except for the one author were naive to the purpose of the experiments. All subjects had normal resolution acuity at all meridians and wore any necessary optical correction. Subjects in all experiments provided informed consent as approved by the University of Louisville's IRB.

2.3. Statistical analysis

For each experiment (Experiments 1, 2.1 and 2.2) a 4-factor repeated-measures ANOVA was applied to the full set of suppression data obtained (see below). In Experiment 1 the four factors were:

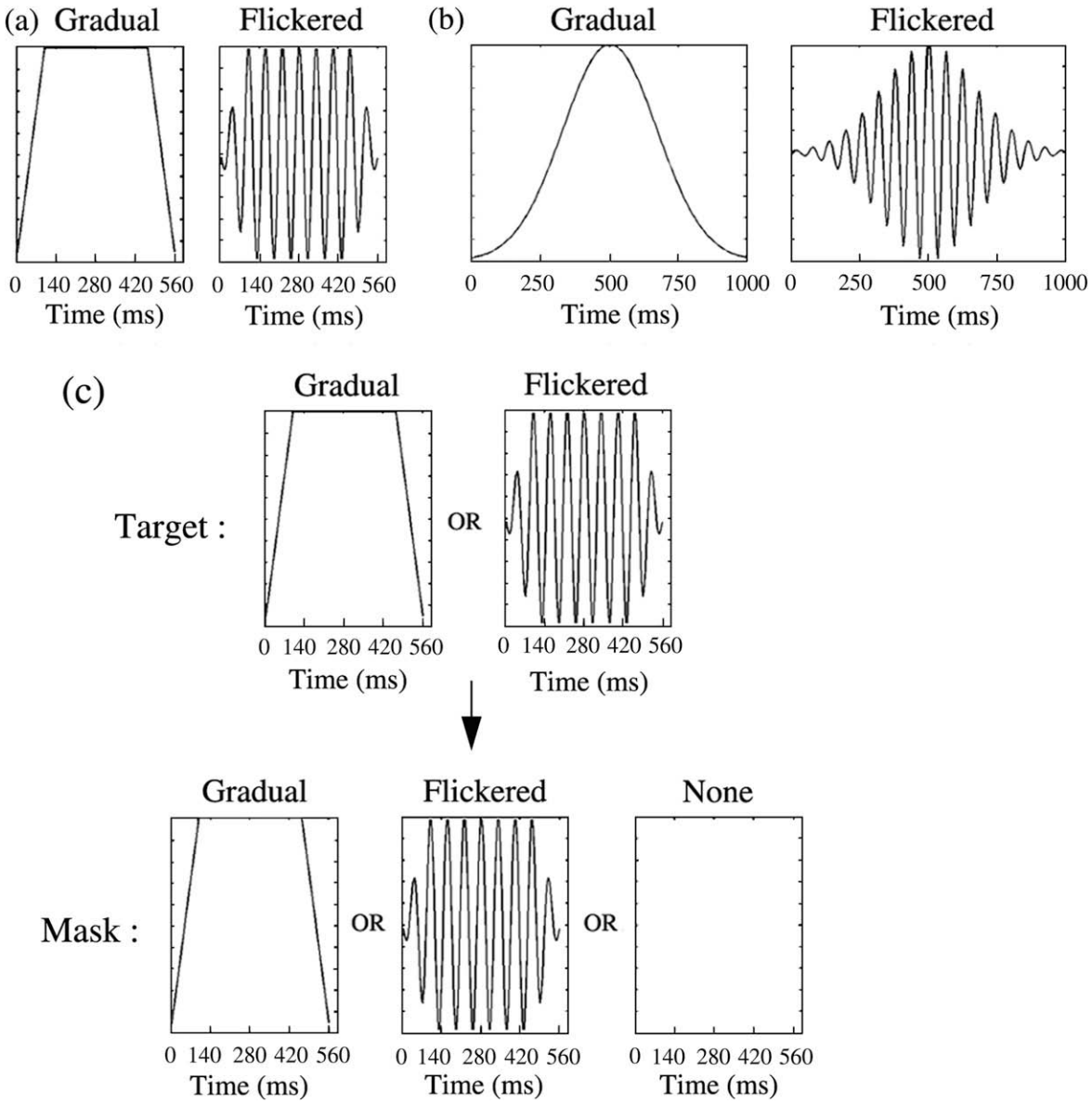

Fig. 2. (a) Two types of temporal envelope, characterized as gradual (ramps and plateau) or flickered (16.7 Hz sinusoid) were used to modulate the contrast of the test and mask stimuli. (b) The temporal envelopes used in Experiment 2 are shown. (c) A summary of the testing conditions used in all experiments is shown. For either the gradual or flickered test target, the mask either matched, mismatched, or was blank (baseline). In Experiment 2, a Gaussian temporal envelope was used rather than the ramp-plateau envelope of Experiment 1 that is shown in 'c'.

test temporal rate (2) × test spatial frequency (2) × matched/mismatched test and mask (2) × test orientation (4). In Experiment 2.1 the four factors were: high-speed/low-speed test (2) × mask configuration (2) × matched/mismatched test and mask (2) × test orientation (4). In Experiment 2.2: high-speed/low-speed test (2) × eccentricity (2) × matched/mismatched test and mask (2) × test orientation (4). When the interactions and/or main effects were significant, orientation differences were pursued further with planned contrasts comparing suppression at horizontal to suppression at oblique orientations (i.e., 45° and 135° combined). All inferential statistics were performed with SPSS version 14.0.

3. Experiment 1: anisotropies in temporally-distinct masking pools

Experiment 1 investigated anisotropic (horizontal effect) masking by a broadband mask with respect to temporal properties. We evaluated whether broadband masking, and specifically anisotropic masking, is observed for both gradual and flickered test gratings at both low and high spatial frequencies, and whether this broadband masking is temporally tuned (i.e., whether both gradual and flickered masks only influence tests with corresponding temporal properties).

Fig. 2a shows the gradual or flickered temporal waveforms used to modulate the contrast of the test and mask stimuli. Test stimuli were sinewave gratings, either 1 or 8 cpd, Gaussian windowed to a 2° width at half height at one of four orientations (0°, 45°, 90°, 135° clockwise from vertical), presented foveally. The test grating was presented with either a gradual or a flickered temporal pattern. Each of these four stimuli was masked by either the (5° diameter) noise mask with a gradual or flickered temporal pattern, or by no mask (i.e., baseline condition) as shown in Fig. 2c.

3.1. Results and discussion

Contrast thresholds for the grating target presented with a gradual temporal waveform are shown in Fig. 3a and target thresh-

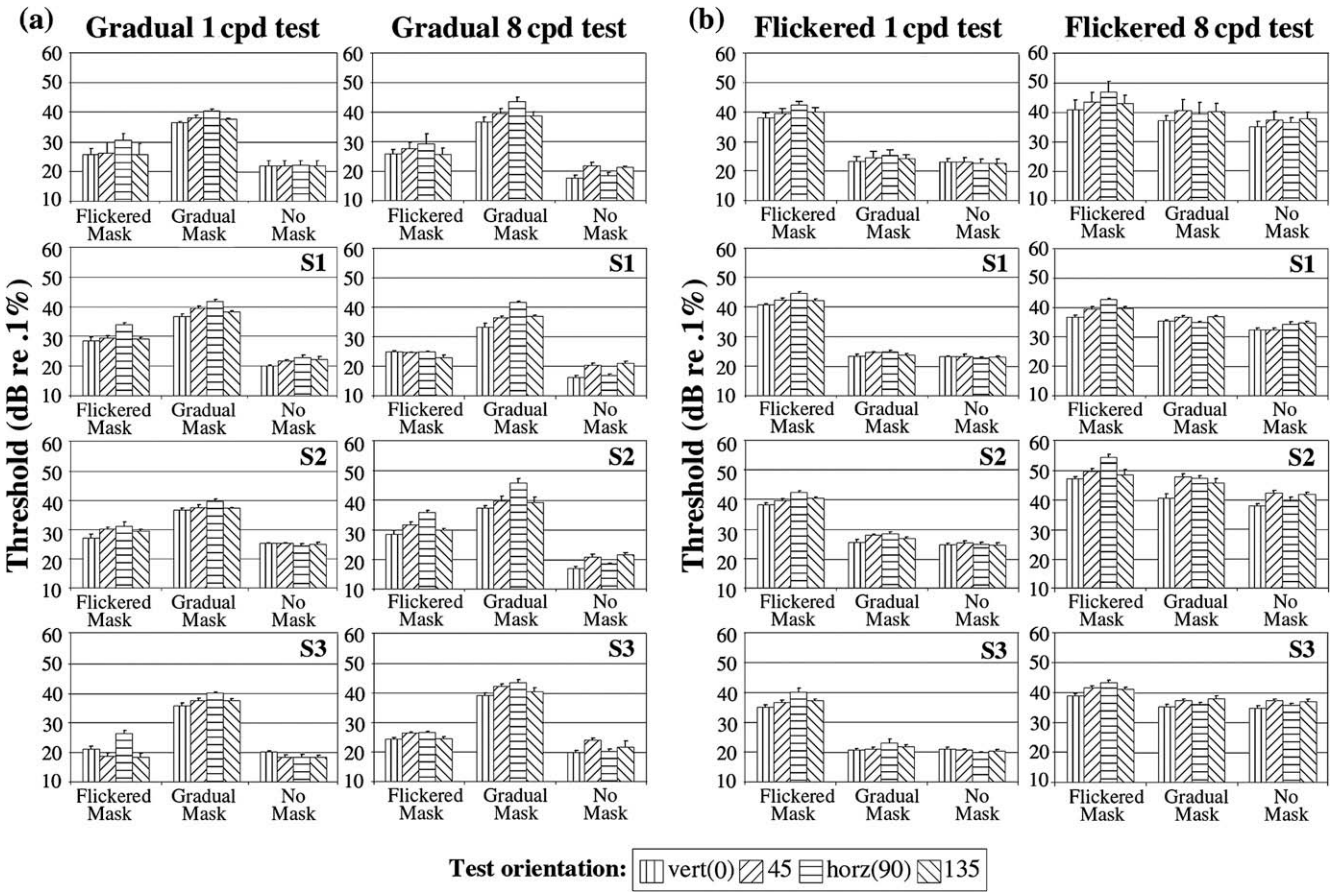

Fig. 3. (a) Contrast thresholds for gradual 1 and 8 cpd test targets at each of four orientations obtained in the presence of either a gradual, or flickered mask, or no mask (baseline). Threshold is expressed in decibels relative to 0.1% contrast. The average of the three subjects is shown in the top row. Error bars are ±1 standard error of the group mean. Individual data are shown in the lower three rows (±1 standard error of the mean of the six replications is shown). (b) Same as 'a' but thresholds are for flickered targets.

olds obtained with the flickered temporal waveform are shown in Fig. 3b. All individual data are shown, with means shown in the top row of the figure. As to be expected, the baseline (no mask) condition shows an oblique effect of contrast threshold at the higher spatial frequency (i.e., highest thresholds are at oblique orientations). However, *masked* contrast thresholds are seen to be highest when the test is horizontal for every subject in most every condition. To show the effects of the 1/*f* noise masks more directly, *suppression factor* was calculated (masked/unmasked thresholds) and is shown in Fig. 4. When the temporal properties of the test and mask match, suppression is very strong, as high as a factor of 19.0, and when the test and mask do not match, suppression is weak or absent, averaging 1.8 (match/mismatch main effect: $F(1, 2) = 144.34$, $p = .007$). Suppression is clearly anisotropic (orientation main effect: $F(3, 6) = 40.53$, $p = .000$) following a horizontal effect pattern with suppression for horizontal targets significantly greater than for oblique targets (planned contrast, $F(1, 2) = 43.71$, $p = .022$). Table 1 shows the suppression factors obtained at each orientation in each condition. To provide a metric of the horizontal effect, an index, Horizontal Effect Index (HEI), was created to express the horizontal effect in suppression factor as a proportion of the general amount of suppression (taken as suppression at obliques) in a given condition. HEI was calculated as the difference of suppression factor at horizontal and oblique orientations divided by the suppression factor for obliques ($HEI = (SF_h - SF_{ob})/SF_{ob}$). These HEI values are shown under each corresponding histogram in Fig. 4, where the HEI can be seen to vary between 0.04 and 1.44 indicating that suppression at horizontal is 4–144% greater than suppression at obliques. That is, suppression at horizontal can be very much larger than suppression at obliques – as much as 2.5 times larger in certain conditions. The HEI (Fig. 4) shows that the horizontal effect is observed broadly across these spatio-temporal conditions.

With respect to spatial frequency (for matching tests and masks), consistent with prior reports using grating masks (e.g., Hess & Snowden, 1992), with the flickered test, suppression is far greater at the lower (1 cpd) spatial frequency than at the higher spatial frequency (an average of 7.6 and 2.3, respectively) whereas with the gradual test, suppression is greater at the higher (8 cpd) spatial frequency than the lower spatial frequency (10.9 and 7.0, respectively). Follow-up analysis of the significant match/mismatch × spatial frequency × temporal rate interaction ($F(1, 2) = 60.21$, $p = .016$) showed that this observation of temporal rate interacting with spatial frequency was significant when test and background match ($F(1, 2) = 42.07$, $p = .023$), but not when they don't match ($F(1, 2) = .288$, N.S.). Strong suppression is seen at both the most low-speed (i.e., gradual, high spatial frequency) and high-speed (flickered, low spatial frequency) conditions. For the gradual test grating with the gradual mask, although much reduced from the 8 cpd, optimal, condition, there is also clear suppression at the lower spatial frequency (1 cpd), suggesting a relation of suppression magnitude to contrast sensitivity. Here, with a gradual presentation, the spatial contrast sensitivity function is bandpass (i.e., better contrast sensitivity at 8 cpd, but still high at 1 cpd), whereas with a rapidly flickering presentation, the contrast sensitivity function is lowpass. Indeed, the amount of sup-

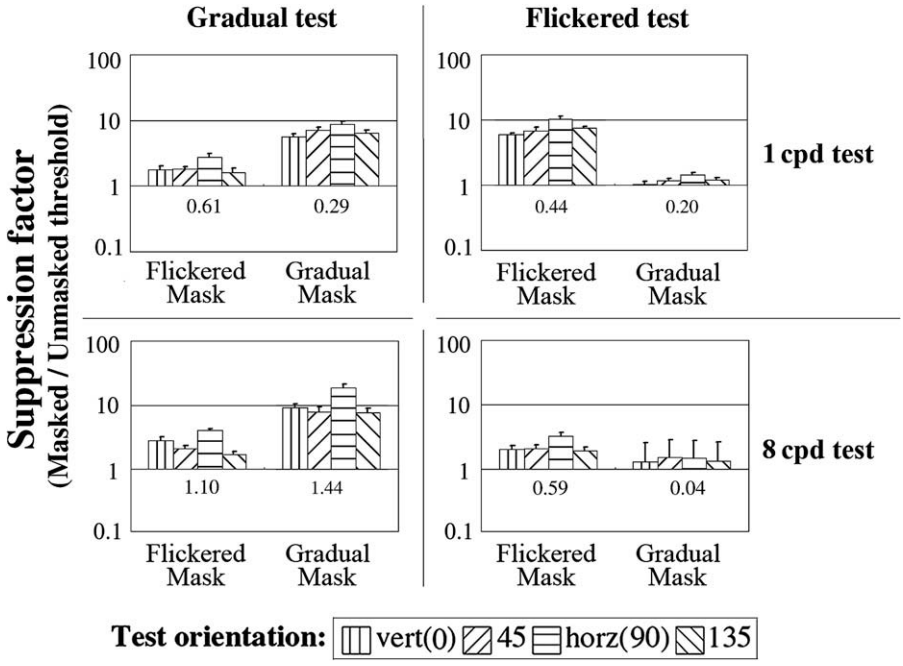

Fig. 4. Suppression factor (the ratio between masked and unmasked threshold) is shown for mean thresholds (top row of Fig. 3). Values greater than 1.0 indicate masking. The individual subjects' standard errors were calculated in terms of Gaussian error propagation (Lo, 2005) and the mean of these standard errors are shown. The magnitude of the horizontal effect, Horizontal Effect Index (HEI), is indicated under the histogram bars for each condition (the difference in suppression at horizontal and at oblique orientations expressed as a proportion of the general level of suppression at that test condition).

Table 1
Mean suppression factors obtained at each orientation in each condition.

Exp. 1	Gradual test								Flickered test							
	Flickered mask				Gradual mask				Flickered mask				Gradual mask			
	Vert.	45	Hori.	135	Vert.	45	Hori.	135	Vert.	45	Hori.	135	Vert.	45	Hori.	135
1 cpd test	1.77	1.79	2.75	1.62	5.71	7.08	8.72	6.44	5.89	6.87	10.28	7.39	1.04	1.17	1.42	1.18
8 cpd test	2.79	2.13	4.01	1.70	9.16	8.01	18.96	7.54	2.03	2.09	3.21	1.92	1.29	1.51	1.49	1.35

Exp. 2.1	Overlay mask								Surround mask							
	Flickered mask				Gradual mask				Flickered mask				Gradual mask			
	Vert.	45	Hori.	135	Vert.	45	Hori.	135	Vert.	45	Hori.	135	Vert.	45	Hori.	135
Flickered 1 cpd test	10.01	9.28	12.07	9.47	0.92	0.90	1.00	0.99	1.07	1.12	1.17	1.15	0.99	0.99	1.04	0.97
Gradual 8 cpd test	1.80	1.51	2.32	1.51	9.96	6.63	12.53	6.99	0.93	0.88	1.06	0.95	0.94	1.02	1.01	0.87

Exp. 2.2	Surround mask															
	0° Eccentricity								2° Eccentricity							
	Flickered mask				Gradual mask				Flickered mask				Gradual mask			
	Vert.	45	Hori.	135	Vert.	45	Hori.	135	Vert.	45	Hori.	135	Vert.	45	Hori.	135
Low s.f. flickered	1.03	1.05	1.17	1.02	1.02	1.02	0.99	1.05	1.48	1.71	2.58	1.48	0.99	0.97	1.06	0.91
High s.f. gradual	0.96	1.09	1.24	1.11	1.11	1.17	1.22	1.07	1.27	1.15	1.34	1.19	1.51	1.17	2.66	1.36

pression observed is highly correlated with baseline contrast sensitivity – suppression ratio approximates a constant factor of contrast sensitivity (here, 8.2%), which fits well with a divisive gain control account of this suppression.

Suppression is highly specific, as noted above, and the magnitude of suppression of a flickered target by a gradual mask, or of a gradual target by a flickered mask, is far less than when the test and mask match in temporal properties. The suppression in these "mismatched" conditions is a factor on the order of 1.2–2.7 (flickered test: 1.2 and 1.4; gradual test: 2.0 and 2.7, for 1 and 8 cpd, respectively). This residual suppression indicates that for a given mechanism detecting a target, the associated masking process is temporally selective but broad enough that it still receives some input at the temporal values of a "mismatched" mask, in the 'tails' of its tuning function.[2] This finding is consistent with the temporal tuning of the gain-control pools demonstrated previously for grating masks (e.g., Hess & Snowden, 1992; Fredericksen & Hess, 1998).

In sum, these results show that the effect of a $1/f$ broadband noise mask is selective (tuned) in the temporal domain. In terms of gain-control processes, these results show that there are sepa-

[2] A control experiment with a very long (2-s) Gaussian envelope, and hence a narrower temporal frequency spectrum, gave comparable results (suppression factors) as with the slowly ramped envelope used here.

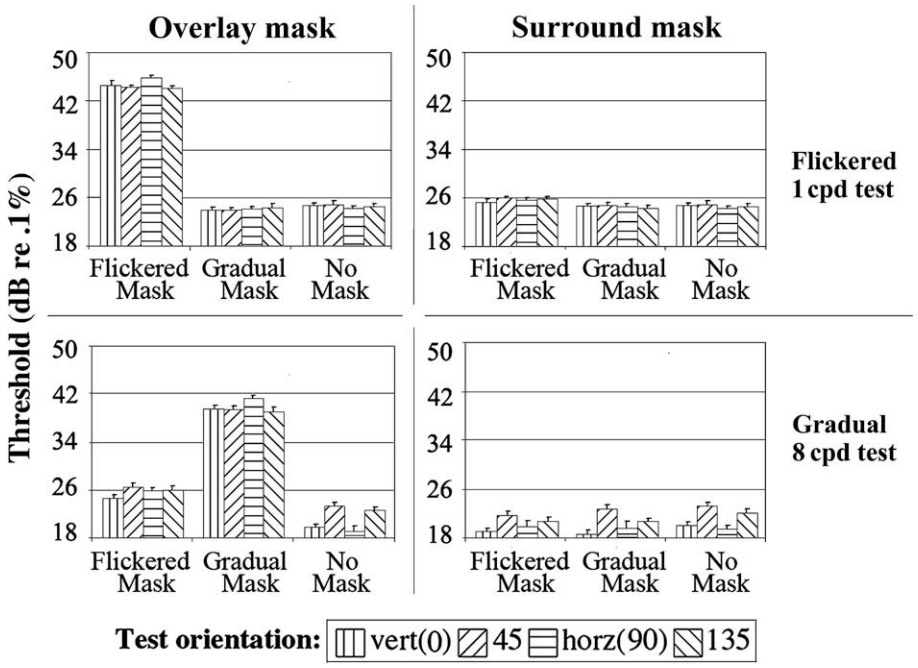

Fig. 5. Data from Experiment 2.1. Mean contrast thresholds for the flickered 1 cpd or gradual 8 cpd test (top row and bottom row, respectively) presented with either an overlay mask (left side) or surround mask (right side) that itself was flickered (left columns) or gradual (middle columns), or absent (right columns).

rate gain-control pools for detecting-mechanisms that differ considerably in spatio-temporal values and each of these pooling processes is anisotropic, showing a horizontal effect.

4. Experiment 2: anisotropic overlay and surround suppression

At fixation, contrast threshold elevation is normally significant only for overlaid masks. However, under certain conditions, surround masking is also reliably measurable at fixation (e.g. Chen & Tyler, 2002; Chen & Tyler, 2008), though it is much more pronounced and easier to obtain in the periphery (Petrov et al., 2005). Since our stimuli in these experiments (Experiment 1 and previous studies) have been large enough to be considered at least partially extra-foveal (they extended 2.5° or more in every direction from fixation), it is possible that surround suppression as well as overlay suppression might play a significant role in the suppression we've measured to date. Thus, the anisotropy observed previously might stem from either, or both, type of suppression. In this experiment we altered test eccentricity and spatial configuration of the mask to measure broadband masking in conventional conditions for eliciting either surround suppression or overlay suppression. In Experiment 2.1 we measured at fixation with the configuration to produce overlay masking and in Experiment 2.2 measured at an eccentric location with a smaller test to produce surround masking.

4.1. Experiment 2.1: Broadband overlay and surround masks tested at fixation

We selected two target conditions from Experiment 1 which produced strong masking effects (low-speed [gradual, 8 cpd] and high-speed [flickered, 1 cpd]), and reproduced these stimuli with smaller tests and with either smaller, target-sized masks (the 'overlay mask' condition; upper row of Fig. 1b), or annular masks with the same outer diameter of the masks in Experiment 1 (the 'surround mask' condition; lower row of Fig. 1b). The inner diameter of the annular masks was 2.37°. To make more area available for the annular surround, and to 'localize' the overlay region, the size of the grating patch was decreased to half from Experiment 1, so at both spatial frequencies the width at half height of the Gaussian spatial window was 1° (Fig. 1b, left column). A fine 1-pixel ring (2.2° in diameter for Experiment 2.1; $3\lambda\sqrt{e}/\sqrt{2}$ for Experiment 2.2), present in both of 2IFC intervals, surrounded the test to decrease the observers' spatial uncertainty (see Petrov, Verghese, & McKee, 2006; Petrov et al., 2005) as shown in Fig. 1b and 1c. We used a Gaussian temporal envelope (duration at half height of 400 ms), that was similar in duration and temporal bandwidth as the ramped envelope used in Experiment 1.[3] Three subjects participated in Experiments 2.1 and 2.2 (with one of the authors and one of the naïve observers participating in both) and two other naïve observers participating in one experiment each.

4.2. Results and discussion

4.2.1. Overall

Fig. 5 shows that thresholds were unaltered from the baseline (no mask) condition by the surround mask (right side) but the overlay mask (left side) is seen to have a pronounced effect on thresholds. Suppression factors (Fig. 6, and Table 1) show that a clear difference in amount of suppression is apparent between overlay and surround configurations ($F(1, 2) = 170.26$, $p = .006$). Furthermore, both configuration × matched/mismatched ($F(1, 2) = 632.15$, $p = .002$) and configuration × matched/mismatched × orientation ($F(3, 6) = 33.15$, $p = .000$) interactions are significant.

4.2.2. Overlay mask

When temporal conditions of the overlay masks and the target gratings matched, large threshold elevations were elicited along with horizontal-effect anisotropies (Fig. 5, left). Suppression factors were as high as 12.5 (Fig. 6), similar to those measured in Experiment 1. However, the mismatched temporal conditions yielded lit-

[3] To confirm this, a control condition was run with this Gaussian temporal envelope and a mask with spatial dimensions identical to those in the first experiment, and obtained results equivalent to those of the corresponding conditions in Experiment 1.

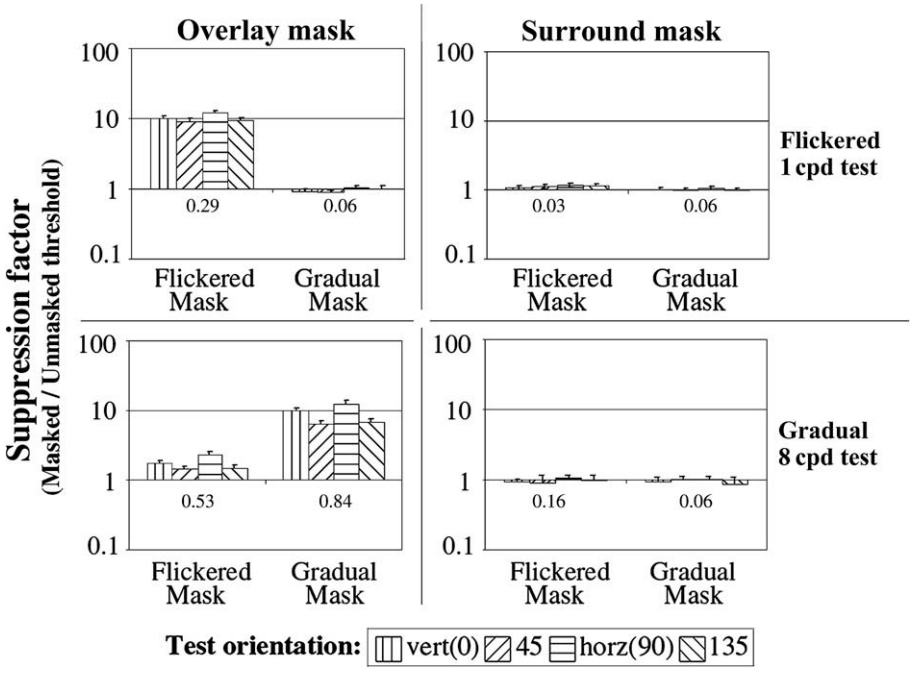

Fig. 6. Suppression factors calculated from the thresholds shown in Fig. 5. Suppression factor values greater than 1.0 indicate masking. Data for overlay masking shown at left; surround masking shown at right. Error bars and HEI as in Fig. 4.

tle (1.8 for the gradual test and flickered mask) or no (1.0 for the flickered test and gradual mask) suppression (matched vs. mismatched within the overlay condition: $F(1, 2) = 508.88$, $p = .002$). For both temporally-matched overlay conditions, horizontal effect patterns of threshold (Fig. 5) were plainly evident leading to significantly greater suppression at horizontal (Fig. 6) with an average suppression factor of 12.30 for horizontal compared to an average oblique suppression factor of 8.10 (planned contrasts, $F(1, 2) = 498.78$, $p = .002$). As in Experiment 1, the largest HEI was obtained for the gradual 8 cpd test with a temporally-matching mask. The HEI here was 0.84, approaching the value of 1.44 obtained with the larger stimulus in Experiment 1.

4.2.3. Surround mask

With the surround mask, essentially no suppression was obtained (Fig. 6, right, average suppression of 1.0), which for testing at fixation is consistent with prior findings (e.g., Petrov et al., 2005). An oblique effect is obtained in the baseline condition and is essentially unchanged by the addition of the surround mask (Fig. 5, right).

In sum, when standard conditions to elicit overlay suppression at fixation are used, suppression is anisotropic, indicating that at least part of the horizontal-effect anisotropy observed with a larger fixated field (the general-viewing conditions of Experiment 1) is due to overlay masking.

4.3. Experiment 2.2: Surround masking at 2° eccentricity

Next we specifically evaluated the anisotropy of surround suppression. To do this we reconfigured our stimuli to match Petrov et al's (2005) spatial configuration (shown in Fig. 1c), and tested for surround suppression at 2° from fixation (and, for comparison, at fixation). In order to carefully localize an eccentric location, the target size was made smaller. The target stimuli in this condition were much smaller than in the original experiments (full width at half height defined as $\lambda\sqrt{e}/\sqrt{2}$, leaving about 1.5 grating cycles visible). At fixation the 1 and 8 cpd grating patches (and overlay masks) were 1.17° and 0.15° wide at half height (the 8 cpd stimulus configuration is shown in Fig. 1c, to scale with the stimuli for Experiments 1 and 2.1). The annular mask consisted of the $1/f$ broadband noise and was sufficiently large that its content could be considered broadband (2λ° inner diameter, 8λ° outer diameter, e.g. 2° and 8° at fixation for the 1 cpd target). An overlay mask was not used as its small size precluded it from containing a sufficiently broadband $1/f$ distribution of content within the overlay region. Target spatial frequency and stimulus size were scaled according to the magnification factor as described by spf/(1 + ecc°/3) (Rovamon & Virsu, 1979), making the test spatial frequencies at 2° eccentricity 0.6 cpd and 4.8 cpd (corresponding to 1 and 8 cpd at fixation). Scaling was accomplished by changing the viewing distance and moving the fixation point, keeping the proportions of the stimulus constant: for the 8 cpd and 4.8 cpd tests, viewing distances were 192 and 115 cm; for the 1 cpd and 0.6 cpd tests, viewing distances were 81 and 46 cm. As in Experiment 2.1, 'low' spatial frequency targets (1 cpd and 0.6 cpd) were flickered at 16.7 Hz, while 'high' spatial frequency targets (8 cpd and 4.8 cpd) were presented with a 400 ms Gaussian temporal envelope.

4.4. Results and discussion

Results show that as in Experiment 2.1, for fixated targets the surround masks had essentially no effect on threshold (Fig. 7, left). Suppression factor (Fig. 8, left, and Table 1) was very close to a factor of 1.0 (1 cpd: 1.1 and 1.0; 8 cpd: 1.2 and 1.1, matching and mismatching, respectively).

In contrast to the 0° eccentricity, when the rescaled stimuli were viewed 2° from fixation, marked masking by the surround was present for the matched temporal-profile conditions (eccentricity × matched/mismatched: $F(1, 2) = 22.45$, $p = .042$; a follow-up ANOVA on the matched vs. mismatched at 2° was significant: $F(1, 2) = 29.03$, $p = .033$, while not significant at 0°: $F(1, 2) = 2.41$, $p = .261$). This surround suppression showed a pronounced horizontal-effect anisotropy (planned contrasts, $F(1, 2) = 45.43$,

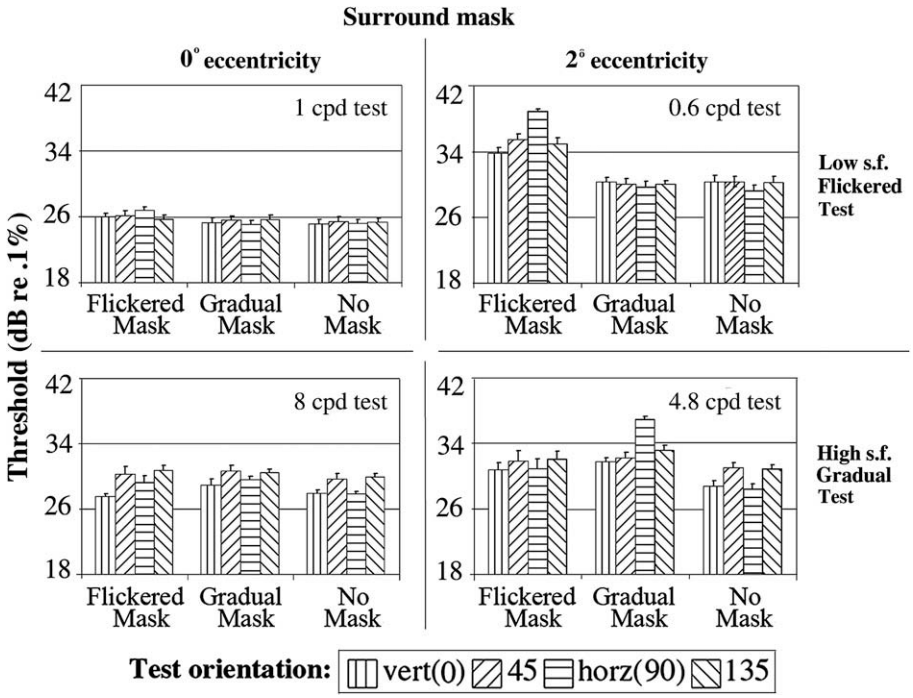

Fig. 7. Data from Experiment 2.2. Mean contrast thresholds for flickered low and gradual high spatial frequency targets tested at fixation (left) or at 2° eccentricity (right) are shown.

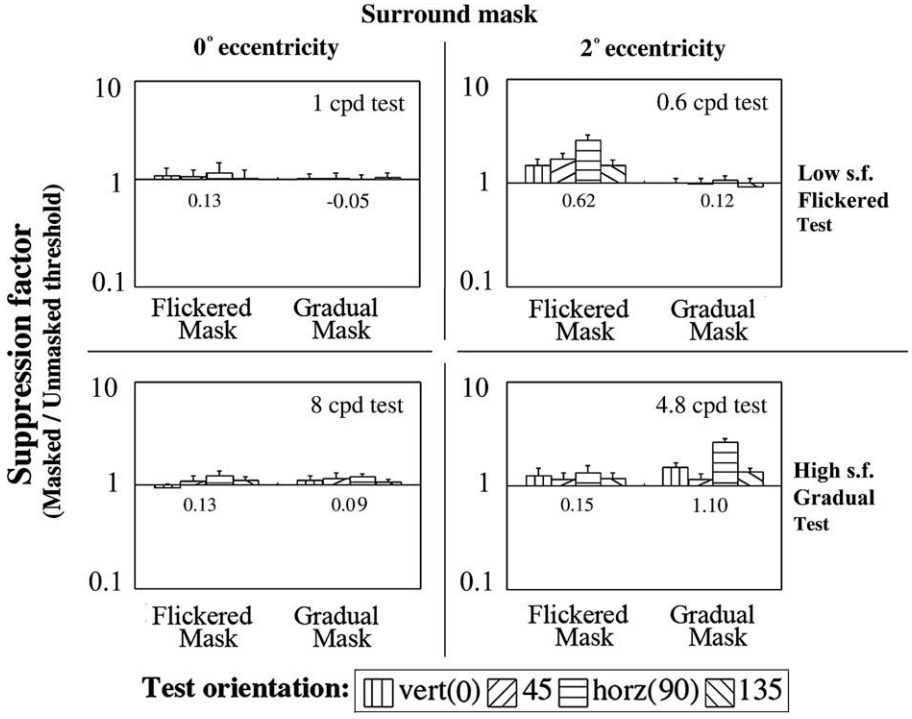

Fig. 8. Suppression factors calculated from the data of Fig. 7. Error bars and HEI as in Fig. 4.

$p = .021$; also the matched/mismatched × eccentricity × orientation interaction was significant: $F(3, 6) = 16.65$, $p = .003$) with suppression factors at horizontal of 2.58 and 2.66, and at obliques of 1.60 and 1.26 for the flickered low spatial frequency and gradual high spatial frequency, respectively. There was little or no suppression in the mismatched conditions (1.0 and 1.2 and for the low and high spatial frequencies, respectively), again showing the temporal tuning of the suppression, here surround suppression. The magnitude of the horizontal effect in the surround suppression demonstrated here was again large (1.10), and, with the particular test conditions used here, intermediate to overlay suppression at fixation (0.84; Experiment 2.1) and to the large 5° stimuli (1.44) for the higher spatial frequency, matching-background, condition (Experiment 2.2).

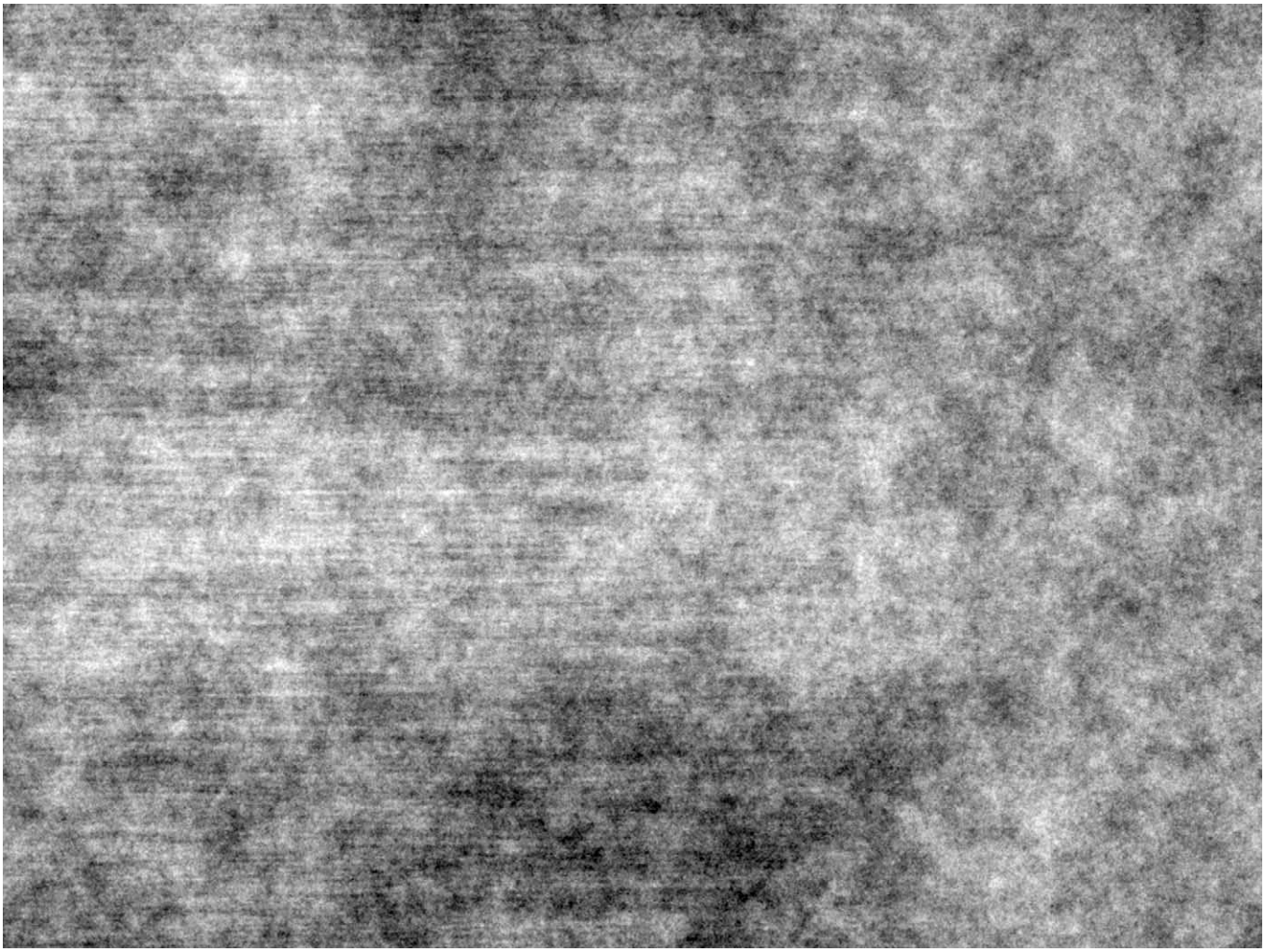

Fig. 9. A replica of a pattern that can be used to demonstrate the horizontal effect (see text and supplementary material). The pattern consists of 1/*f* broadband noise with contrasts incremented within a band of orientations that correspond to the longer axis of the pattern (a 45°-wide orientation band with contrast weighted by a triangle filter; see e.g. Hansen & Essock, 2006). The increment is graded as the square root of distance, diminishing from left to right from +20% at far left to +0% at far right. Spatial frequency content ranges from 1 cpp to as high as 512 cpp, though the limit will be determined by print and display resolution.

In sum, surround suppression is also anisotropic. Both surround suppression and overlay suppression will contribute to the horizontal-effect anisotropy that occurs in broadband masking when spatial stimulus conditions are appropriate, such as in viewing a typical every-day scene.

5. Conclusions

The horizontal effect is ubiquitous. The anisotropy is seen in conditions that produce overlay suppression *and* those that produce surround suppression, as well as 'general viewing' conditions with a large fixated field. The anisotropy is seen at a variety of spatio-temporal conditions including both high-speed and low-speed mechanisms (i.e., relatively sustained and transient temporal mechanisms). Thus, in the variety of conditions tested here and in previous reports, the suppression of a spatial filter detecting content in the context of a range of other spatial structure is strongest at horizontal orientations and weakest at oblique orientations.

Comparison of the results for when the temporal properties of the test and background match to when they are mismatched further affirms that the anisotropic suppression is caused by a process that responds relatively locally (i.e., relatively local in the frequency domain) to broadband content (e.g., Cass & Alais, 2006; Fredericksen & Hess, 1998). When contextual structure is present to drive numerous detectors, the pooled activity of spatio-temporally similar detectors is adequate to reveal the anisotropic nature of this suppressive process that we show to be tuned in temporal frequency as well as in spatial frequency and orientation (Essock, Hansen, & Haun, 2007; Essock et al., 2009). Although similar to the temporal tuning evoked by a narrowband mask (e.g., Boynton & Foley, 1999), the tuned suppression demonstrated with broadband masks is even more clearly tied to the temporal parameters of the test (Kim & Essock, 2010). Here we show that these relatively-local gain-control pools are anisotropic, all showing a horizontal effect.

Meese and Holmes (2007) have shown that overlay suppression by an orthogonal grating ("cross-orientation" masking) is very strong at high speeds (i.e., at high temporal rates and low spatial frequencies) and that this cross-orientation masking is absent at low speeds (see also, Medina & Mullen, 2009; Cass & Alais, 2006; Meese & Baker, 2008; Meese & Hess, 2004; Meier & Carandini, 2002) and that this is particularly true for monoptic suppression (Meese & Baker, 2009). Because of the differential behavior, they suggested that the high-speed and low-speed processes might reflect distinctly organized channels, specifically the activity of M and P cells, respectively. Furthermore, they suggest (Meese & Baker, 2009) that the relation of masking to speed stems from a monoptic, subcortical mechanism and is directly based on the ratio of M- to

P-cell activity. Such a speed relation is not seen here in the overlay data most likely because our broadband mask did not contain fully orthogonal content (confined here to ±7.5° from the test), although there was some suggestion of this relation in Experiment 1. However, to the extent that speed distinguishes mediation by M and P cell types, or to the extent that our relatively transient and sustained test conditions reflect the activity of the cell types differentially, the present results indicate that suppressive mechanisms mediated by both cell types show anisotropic gain control. The present results do not address how many gain-control pools exist across the spatio-temporal surface, but do show that there are more than two fixed pools (Experiment 1) and that all are anisotropic (at the spatio-temporal values tested). Indeed, it is likely that each detecting-mechanism has its own pool (cf. Foley, 1994; Wainwright, Schwarz, & Simoncelli, 2001), weighted anisotropically as a function of orientation.

Although one may at first wonder if this effect might simply reflect a bias inherent in a CRT display, for several reasons it is clear that this anisotropy is not an artifact. First, this is a large effect that is perceptually obvious when viewing suprathreshold structure. An increment of amplitude of broadband structure at a given band of orientations (e.g., see examples in Fig. 1 in Hansen & Essock, 2004, or Fig. 1 in Essock et al., 2003) is clearly most pronounced at oblique orientations, least pronounced at horizontal and intermediate at vertical. Moreover, if such a pattern is printed and rotated, this effect is immediately seen to not be tied to the pattern's orientation on the paper but rather to the retinal (or gravitational) coordinates, showing that the anisotropy in the salience of oriented structure is not associated with the orientation of the display (in this case, the paper). The supplementary material provides a pattern that can be printed and used to demonstrate this (Fig. 9 shows a small version for illustrative purposes). If one prints this pattern, it can be readily rotated providing a physically-identical pattern viewed at different test orientations. If the pattern is first held without rotation, the salience of the oriented structure at the high-contrast end (left) can be noted and when then rotated 45° a dramatic increase in the salience of the oriented structure will be apparent. Examination of this suprathreshold oriented structure at the high-contrast-increment end of the pattern (left, as printed) and comparison to the observed saliency of this suprathreshold oriented structure when the pattern is rotated to a variety of other orientations will reveal the horizontal effect of structure salience.[4] Although not as dramatic, the horizontal effect that exists at detection threshold can also be demonstrated by the printed pattern. By carefully noting the physical point along the gradient when the oriented nature of the structure is no longer clear, then comparing this point when the page is rotated to various orientations, the threshold difference can be approximated.

The second factor indicating that the horizontal effect is not a stimulus artifact associated with a CRT display is that if different stimulus orientations are produced by physically rotating the display monitor, rather than by changing the stimulus on the monitor raster, the anisotropy of detection thresholds follows the retinal orientation of the pattern, not the orientation of the monitor. This control condition has been measured and reported for contrast threshold of a grating on a broadband mask (Essock et al., 2009) as well as detection and increment threshold for a broadband oriented pattern (Essock et al., 2003). In other words, whatever effect anisotropies inherent in a monitor's raster have on thresholds is vastly outweighed by this anisotropic visual bias that we report. Third, the present experiment obtained the anisotropy at 2° retinal eccentricity but not at 0° eccentricity (Experiment 2.2, for conditions testing surround suppression). If the anisotropic findings were due to an anisotropy inherent in CRT monitors, it would have caused anisotropic performance at both retinal eccentricities as the stimuli in both conditions were presented at the same location on the same monitor in the same fashion (i.e., only the fixation point was changed). Finally, direct measurement of the luminance of the bright and dark bars of the 1 cpd pattern at different orientations on the raster show absolutely no difference at different orientations (IL1700 photometer, International Light, Inc.).

This anisotropy has pragmatic implications for interpreting results of masking experiments. Experiments intending to measure one type of masking may find effects of different size, or even no measurable effect at all, at certain spatio-temporal conditions simply on the basis of whether the target is vertical or horizontal. (Most studies on surround or flanker masking have used vertical targets (e.g. Cannon & Fullenkamp, 1993; Chen & Tyler, 2001), Petrov et al. (2005), Petrov et al. (2006) have used oblique targets, and Meese et al. (2007) have used horizontal targets). Another implication of the anisotropy concerns the origin of overlay suppression. There are suggestions that overlay suppression is an earlier, perhaps even subcortical, type of suppression (e.g., Li, Thompson, Duong, Peterson, & Freeman, 2006; Petrov et al., 2005; Prebe & Ferster, 2006). In the conditions used here, an overlay mask causes a very strong horizontal-effect anisotropy, which would suggest that suppression evoked by the overlay masks in these conditions is unlikely to be dominated by a subcortical process due to the strong orientation properties displayed. If subcortical processes do contribute to overlay masking, then it is very likely that an additional, second, source of overlay masking originates in the cortex (Baker Meese & Summers, 2007; Meese & Baker, 2008, 2009; see also Cass, Stuit, Bex, & Alais, 2009).

[4] Note how the salience diminishes when a given orientation is first viewed and how the diminution is least at oblique orientations and most at horizontal. This initial decline of salience is presumably due to the relatively slow nature of gain control and its perceptual consequences (e.g., Bonds, 1991; Khang & Essock, 2000).

Acknowledgments

Supported by Grant # N00014-03-1-0224 from the Office of Naval Research and Kentucky Space Grant Consortium – NASA.

Appendix A. Supplementary data

Supplementary data associated with this article can be found, in the online version, at doi:10.1016/j.visres.2010.01.020.

References

Anderson, S. J., & Burr, D. C. (1985). Spatial and temporal selectivity of the human motion detection system. *Vision Research, 25*, 1147–1154.
Baker, D. H., Meese, T. S., & Summers, R. J. (2007). Psychophysical evidence for two routes to suppression before binocular summation of signal in human vision. *Neuroscience, 146*, 435–448.
Bex, J. P., Verstraten, F. A. J., & Mareschal, I. (1996). Temporal and spatial frequency tuning of the flicker motion aftereffect. *Vision Research, 36*, 2721–2727.
Bonds, A. B. (1991). Temporal dynamics of contrast gain in single cells in the cat striate cortex. *Visual Neuroscience, 6*, 239–255.
Boynton, G. M., & Foley, J. M. (1999). Temporal sensitivity of human luminance pattern mechanisms determined by masking with temporally modulated stimuli. *Vision Research, 39*, 1641–1656.
Cannon, M. W., & Fullenkamp, S. C. (1993). Spatial interactions in apparent contrast: Individual differences in enhancement and suppression effects. *Vision Research, 33*, 1685–1695.
Cass, J., & Alais, D. (2006). Evidence for two interacting temporal channels in human visual processing. *Vision Research, 46*, 2859–2868.
Cass, J., Stuit, S., Bex, P., & Alais, D. (2009). Orientation bandwidths are invariant across spatiotemporal frequency after isotropic components are removed. *Journal of Vision, 9*, 1–14.
Chen, C. C., & Tyler, C. W. (2001). Lateral sensitivity modulation explains the flanker effect in contrast discrimination. *Proceedings of the Royal Society of London B: Biological Sciences, 268*, 509–516.
Chen, C. C., & Tyler, C. W. (2002). Lateral modulation of contrast discrimination: Flanker orientation effects. *Journal of Vision, 2*, 520–530.
Chen, C. C., & Tyler, C. W. (2008). Excitatory and inhibitory interaction fields of flankers revealed by contrast-masking functions. *Journal of Vision, 8*, 1–14.

Essock, E. A., DeFord, J. K., Hansen, B. C., & Sinai, M. J. (2003). Oblique stimuli are seen best (not worst!) in naturalistic broad-band stimuli: A horizontal effect. *Vision research, 43*, 1329–1335.

Essock, E. A., Hansen, B. C., & Haun, A. M. (2007). Perceptual bands in orientation and spatial frequency: A cortical analogue to Mach bands. *Perception, 36*, 636–649.

Essock, E. A., Haun, A. M., & Kim, Y. J. (2009). Anisotropy of orientation-tuned suppression that matches the anisotropy of typical natural scenes. *Journal of Vision, 9*, 1–15.

Foley, J. M. (1994). Human luminance pattern-vision mechanisms: masking experiments require a new model. *Journal of the Optical Society of America A, Optics, Image Science, and Vision, 11*, 1710–1719.

Fredericksen, R. E., & Hess, R. F. (1998). Estimating multiple temporal mechanisms in human vision. *Vision Research, 38*, 1023–1040.

Fredericksen, R. E., & Hess, R. F. (1999). Temporal detection in human vision: dependence on spatial frequency. *Journal of the Optical Society of America A, 16*, 2601–2611.

Hammett, S. T., & Snowden, R. J. (1995). The effect of contrast adaptation on briefly presented stimuli. *Vision Research, 35*, 1721–1725.

Hansen, B. C., Essock, E. A., Zheng, Y., & DeFord, J. K. (2003). Perceptual anisotropies in visual processing and their relation to natural image statistics. *Network: Computation in Neural Systems, 14*, 501–526.

Hansen, B. C., & Essock, E. A. (2004). A horizontal bias in human visual processing of orientation and its correspondence to the structural components of natural scenes. *Journal of Vision, 4*(12), 1044–1060.

Hansen, B. C., & Essock, E. A. (2005). Influence of scale and orientation on the visual perception of natural scenes. *Visual Cognition, 12*, 1199–1234.

Hansen, B. C., & Essock, E. A. (2006). Anisotropic local contrast normalization: The role of stimulus orientation and spatial frequency bandwidths in the oblique and horizontal effect perceptual anisotropies. *Vision Research, 46*, 4398–4415.

Haun, A. M., & Essock, E. A. (in preparation). Anisotropies of contrast sensitivity in 1/*f* noise.

Hess, R. F., & Snowden, R. J. (1992). Temporal properties of human visual filters: Number, shapes and spatial covariation. *Vision Research, 32*, 47–59.

Khang, B. G., & Essock, E. A. (2000). Apparent swinging motion from a 2-D sinusoidal pattern. *Perception, 29*, 453–459.

Kim, Y.J., Essock, E.A. (2010). Anisotropic gain control pools are tuned in temporal frequency as well as spatial frequency and orientation. (Abstract) *Journal of Vision, 9*, in press.

Li, B., Thompson, J. K., Duong, T., Peterson, M. R., & Freeman, R. D. (2006). Origins of cross-orientation suppression in the visual cortex. *Journal of Neurophysiology, 96*, 1755–1764.

Lo, E. (2005). Gaussian error propagation applied to ecological data: post-ice-storm-downed woody biomass. *Ecological Monographs, 75*, 451–466.

Mandler, M. B., & Makous, W. (1984). A three channel model of temporal frequency perception. *Vision Research, 26*, 609–619.

Medina, J. M., & Mullen, K. T. (2009). Cross-orientation masking in human color vision. *Journal of Vision, 9*, 1–16.

Meese, T. S., & Baker, D. H. (2008). Spatiotemporal properties of cross-orientation masking: Speed computation precedes ipsiocular suppression, and interocular suppression is scale invariant. *Journal of vision*.

Meese, T. S., & Baker, D. H. (2009). Cross-orienatation masking is speed invariant between ocular pathways but speed dependent within them. *Journal of Vision, 9*, 1–15.

Meese, T. S., & Hess, R. F. (2004). Low spatial frequencies are suppressively masked across spatial scale, orientation, field position, and eye of origin. *Journal of Vision, 4*, 843–859.

Meese, T. S., & Holmes, D. J. (2007). Spatial and temporal dependencies of cross-orientation suppression in human vision. *Proceedings of the Royal Society of London B, 274*, 127–136.

Meese, T. S., Summers, R. J., Holmes, D. J., & Wallis, S. A. (2007). Contextual modulation involves suppression and facilitation from the center and the surround. *Journal of Vision, 7*, 1–21.

Meier, L., & Carandini, M. (2002). Masking by fast gratings. *Journal of Vision, 2*, 293–301.

Petrov, Y., Carandini, M., & McKee, S. P. (2005). Two distinct mechanisms of suppression in human vision. *Journal of Neuroscience, 25*, 8704–8707.

Petrov, Y., Verghese, P., & McKee, S. P. (2006). Collinear facilitation is largely uncertainty reduction. *Journal of Vision, 6*, 170–178.

Prebe, N. J., & Ferster, D. (2006). Mechanisms underlying cross-orientation suppression in cat visual cortex. *Nature Neuroscience, 9*, 552–561.

Rovamon, J., & Virsu, V. (1979). An estimation and application of the human cortical magnification factor. *Experimental Brain Research, 37*, 495–510.

Snowden, R. J. (2001). Contrast gain mechanism or transient channels? Why the effects of a background pattern alter over time. *Vision Research, 41*, 1879–1883.

Wainwright, M. J., Schwarz, O., & Simoncelli, E. P. (2001). Natural image statistics and divisive normalization: Modeling nonlinearity and adaptation in cortical neurons. In R. Rao, B. Olshausen, & M. Lewicki (Eds.), *Probabilistic models of the brain: Perception and neural function*. Cambridge, MA: MIT Press.

Yu, C., Klein, S. A., & Levi, D. M. (2003). Cross- and iso-oriented surrounds modulated the contrast response function: The effect of surround contrast. *Journal of Vision, 3*, 527–540.